Is PSHA an option for earthquake early warning?

I. Iervolino
Dipartimento di Ingegneria Strutturale, Università degli Studi di Napoli Federico II,
Via Claudio 21, 80125, Naples, Italy; email: iunio.iervolino@unina.it.

ABSTRACT: Recent efforts of real-time seismology on rapid assessment of earthquake magnitude and location enable to provide an estimate of the event's features from a few seconds to a few tens of seconds before the ground motion arrives at a specific site. Then, when an event is occurring, probabilistic distributions of magnitude and source-to-site distance are available. Consequently the prediction of the peak ground motion at the site, conditional on the seismic network measures, may be performed in analogy with the probabilistic seismic hazard analysis (PSHA). This results in time-dependent hazard curves which may be used as a support tool for automated decision making in order to reduce the expected loss of specific structures/infrastructures in the framework of performance-based earthquake engineering, even in those cases where limited lead-time renders evacuation unfeasible. However, such prediction is performed in very uncertain conditions which both refer to the real-time estimation of source parameters and traditional uncertainties involved in PSHA.

The objective of this paper is to review the issues related to the real-time adaption of PSHA with the aim to assess whether it may be an adequate tool for earthquake early warning. The investigations include sensitivity analysis of the prediction with respect to the uncertainties involved, with consideration of their time dependency, and the trade-off between the available lead-time and the level of information. Results, in terms of missed and false alarm rates and expected loss reduction, are also discussed with respect to different possible applications of EEW.

1 INTRODUCTION

Earthquake early warning systems (EEWSs) exist and may be classified, by the seismic network configuration, as regional or site-specific. Regional EEWSs typically consist of a number of seismic stations covering a potential source zone. Such systems are designed to provide data that can be used to estimate the main parameters of the event, as time of origin, magnitude and location, and to predict peak ground motion at some other sites in a large area. This processing may require significant time and therefore these systems are mainly devoted to *near-real-time* applications as the well known post-event *shake-maps*.

For critical facilities with a large loss potential, a fence of seismic instruments may be placed around the equipment to protect it. This is the case of site-specific EEW, which reduce the risk connected to the failure of nuclear power plants or lifelines by providing sufficient warning time to take actions to decrease the risk reducing vulnerability and/or exposure. The networks devoted to site-specific EEW are much smaller than those of the regional type, only covering the surroundings of the system. The distance of the seismic instruments from the facility depends on the lead-time (defined as the available time between the alarm and the strike) needed to activate the safety procedures before the arrival of the more energetic seismic phase. In this kind of systems the alarm is typically issued when the ground motion at one or more sensors exceeds a given threshold. In fact, unlike the regional case, site-specific EEWSs only measure the ground shaking at the network and do not attempt to estimate the features of the event, which would require unacceptable computational time. It is also to mention that sometimes the instruments for on-site early warning can be placed within the building, in this case the instrument triggers on the P-waves and the lead-time is provided by the difference between P- and S-wave velocities.

Due to a large development of regional networks in recent years worldwide, and because of the current advances of real-time seismology, the question of using EEWSs for site-specific applications (Figure 1) is rising. Hybrid EEWSs are of current interest as cost-effective solutions for seismic risk mi-

tigation, although efficiency evaluation and feasibility analysis for earthquake engineering applications is still debated. In fact, it will be shown that in the framework of the performance-based earthquake engineering (PBEE) these systems can provide real-time predictions of ground motion intensity measures (IMs) at a site or, for a structure of interest, even the expected loss associated to the strike of the detected earthquake. Nevertheless, such prediction involves significant uncertainty and therefore effectiveness of EEW for engineering applications requires proper assessment.

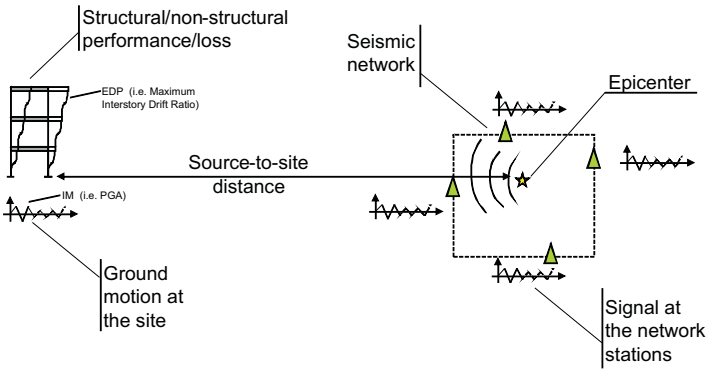

Figure 1. Hybrid EEWS sketch (Iervolino et al., 2006).

This paper presents a review of the work of the author and co-workers about the real-time adaption of probabilistic seismic hazard analysis or PSHA (Cornell, 1968) and of PBEE framework. In particular, the procedure for early warning prediction of engineering ground motion parameters is presented first, then some issues related to the involved uncertainty and its influence on the alarm issuance decision (e.g., false/missed alarm occurrences) are discussed. Secondly, a prototypal terminal based on real-time PSHA and able to issue the alarm for the EEWS under development in the Campania region (southern Italy) is shown. Finally, it is discussed how to set EEW alarm thresholds, for structures and infrastructures, based on the expected loss conditional on the information provided in real-time by the seismic network.

2 REAL-TIME PSHA

Seismologists have recently developed several methods to estimate the magnitude (M) of an event given limited information of the P-waves for real-time applications. Similarly, the source-to-site distance (R) may be rapidly determined by analyzing the time and order of the seismic stations detecting the developing earthquake. Therefore, for earthquake early warning purposes, it is possible to assume that, while the event is still propagating, estimates of M and R are available, and the peak ground motion at the site can be predicted via the probabilistic seismic hazard analysis conditional to the real-time information given by the seismic sensors network (Iervolino et al., 2006).

In fact, assuming that at a given time t from the earthquake's origin, the seismic network can provide a vector of measures informative for the magnitude, $\{\tau_1, \tau_2,\ldots, \tau_n\}$, the posterior probability density function (PDF) of M conditional to the measures, $f(m|\tau_1,\tau_2,...,\tau_n)$, may be obtained via the Bayes theorem, as in Eq. (1):

$$f(m\,|\,\tau_1,\tau_2,...,\tau_n)=\frac{f(\tau_1,\tau_2,...,\tau_n\,|\,m)f(m)}{\int_{M_{\min}}^{M_{\max}} f(\tau_1,\tau_2,...,\tau_n\,|\,m)f(m)dm} \quad (1)$$

In the Bayesian framework $f(m)$, the *a priori* distribution, is used to incorporate the information available before the seismic network performs the measurements. Then, in this application, a natural candidate for $f(m)$ is the truncated exponential of Eq. (2), derived by the Gutenberg-Richter relationship typically used in the classic hazard analysis. $\{\beta, M_{\min}, M_{\max}\}$ are dependent on the seismic features of the region under study and will be assumed for the Campania region equal to $\{1.69, 4, 7\}$.

$$f(m)=\begin{cases}\dfrac{\beta e^{-\beta m}}{e^{-\beta M_{\min}}-e^{-\beta M_{\max}}} & M_{\min}\le m\le M_{\max}\\ 0 & m\notin[M_{\min},M_{\max}]\end{cases} \quad (2)$$

The joint PDF $f(\tau_1,\tau_2,...,\tau_n\,|\,m)$ is the *likelihood* function. It is used to incorporate into the analysis all information on M contained into the real-time data. Under the hypothesis that the τ measurements are s-independent and identically distributed lognormal random variables it may be formulated as in Eq. (3).

$$f(\tau_1,\tau_2,...,\tau_n\,|\,m)= =\left(\frac{1}{\sqrt{2\pi}\sigma_{\ln(\tau)}}\right)^n\left(\prod_{i=1}^{n}\frac{1}{\tau_i}\right)e^{\left(-\frac{\sum_{i=1}^{n}(ln(\tau_i))^2}{2\sigma^2_{\ln(\tau)}}+\frac{2\mu_{\ln(\tau)}\left(\sum_{i=1}^{n}ln(\tau_i)\right)-n\mu^2_{\ln(\tau)}}{2\sigma^2_{\ln(\tau)}}\right)} \quad (3)$$

The parameters in Eq. (3) may be, for example, the mean, $\mu_{\ln(\tau)}$, and the standard deviation, $\sigma_{\ln(\tau)}$, of the log of the predominant period of the first four seconds of the P-waves retrieved from the study of Allen and Kanamori (2003), Eq. (4).

$$\begin{cases} \mu_{\ln(\tau)} = (M - 5.9)/(7\log(e)) \\ \sigma_{\ln(\tau)} = 0.16/\log(e) \end{cases} \quad (4)$$

Combining Eq. (3) and Eq. (2) into Eq. (1), the posterior PDF of the magnitude results that of Eq. (5), which depends on the measures only via the summation of the logs, $\sum_{i=1}^{n} \ln(\tau_i)$. The λ constant of Eq. (5) is given in Eq. (6) and may be evaluated numerically[1].

$$f(m \mid \tau_1, \tau_2, ..., \tau_n) = \lambda \cdot e^{-\beta m + \left(2\mu_{\ln(\tau)}\left(\sum_{i=1}^{n} ln(\tau_i)\right) - n\mu^2_{\ln(\tau)}\right)/2\sigma^2_{\ln(\tau)}} \quad (5)$$

$$1/\lambda = \int_{M_{\min}}^{M_{\max}} e^{-\beta m + \left(2\mu_{\ln(\tau)}\left(\sum_{i=1}^{n} ln(\tau_i)\right) - n\mu^2_{\ln(\tau)}\right)/2\sigma^2_{\ln(\tau)}} dm \quad (6)$$

Regarding the source-to-site distance, because of rapid earthquake localization procedures, a probabilistic estimate of the epicenter may also be available. For example, during an earthquake the RTLoc algorithm (Satriano et al., 2008) allows to assign to each point of a grid, defined in the region where the network operates, the probability that the hypocenter is coincident with that point based on the sequence according to which the stations trigger, $\{s_1, s_2, \ldots, s_n\}$. Consequently, also the PDF of R, $f(r|s_1,s_2,...,s_n)$, may be retrieved in real-time. Thus, it is possible to compute the probabilistic distribution (or hazard curve[2]) of a ground motion intensity measure at a site of interest as in Eq. (7), which also requires an attenuation relationship, $f(im|m,r)$, available for the chosen IM. This procedure will be referred to as RTPSHA and may be used to predict, for example, of peak ground acceleration (PGA) or spectral ordinates (Convertito et al., 2008).

$$f_n(im) = \int_m \int_r f(im|m,r)\ f(m|\tau_1,\tau_2,...,\tau_n) \times \times f(r|s_1,s_2,...,s_n)\ dr\ dm \quad (7)$$

2.1 *Example of RTPSHA for the Campanian EEWS.*

ISNet is a network of 29 strong motion seismic stations deployed in a 100x70km^2 area covering the epicentral location of the main earthquakes that occurred in the southern Appennines in Italy (Weber et al., 2007). The EEWS under development in Campania using ISNet has been designed to be of the hybrid type discussed above, i.e., a seismic network, located where the large earthquakes are likely to occur, has the potential to protect several critical structures/infrastructures at the same time. The way the ISNet EEWS operates may be represented by three blocks, which may also be simulated to provide an example of how RTPSHA works:

1. ***Acquisition.*** Given the basic features of the earthquake (i.e., the *true* values of magnitude and location), the τ measurements for the triggered stations are needed to perform the RTPSHA. The stations' measurements may be simulated sampling from the $f(\tau \mid m)$ distribution. In the simulation process, the number and sequence of stations triggered is also computed assuming an appropriate velocity model for the region; this gives evolutionary information on the location of the earthquake.

2. ***Computation***. This block furnishes evolving real-time estimates of the hypocenter (i.e., the distance of the source from the site for which the prediction of peak ground motion is sought) and the magnitude of the earthquake as described in section 2. At each 1 sec time step, the estimates of R and M are updated on the basis of new information collected by the network.

3. ***Decision***. The hazard integral of Eq. (7) is computed, i.e., the prediction of the IM at the target site is obtained and the decision whether to issue an alarm or not is taken. The alarm issuance implies a decisional rule. For example, assuming that the predicted IM is the PGA, a simple one consists of issuing the alarm if the risk that the critical peak ground motion value (PGA_c) will be exceeded in the strike, is larger than a probability threshold (P_c), Eq. (8). Probabilistic procedures that can be used to set more effective decisional rules based on the minimization of the expected loss for structures and infrastructures, are reviewed in the following.

$$P[PGA > PGA_c] > P_c \quad (8)$$

Results of the simulation of this procedure for a M 6 event located within the ISNet network are given in Figure 2. As a target site, the city of Naples, capital of the Campania region, is considered (Figure

[1] This Bayesian approach to the estimation of magnitude has proven to be more efficient than other simpler approaches based on classical point estimates, see Iervolino et al. (2009) for a discussion.

[2] The subscript *n* in the left-hand side of Eq. (7) means that the computed hazard curve refers to a particular set of triggered stations and, therefore, evolves with time.

2a). The probabilistic PDFs of the magnitude are given in Figure 2b. Figure 2c represents the distributions of R. Note that the true distance of Naples from the epicenter of the simulated event, equal to 124km, is well captured by the PDFs. In Figure 1d, the real-time hazard curves are given (the used attenuation relationship is that from Sabetta and Pugliese, 1996) for the target site. In the panels of Figure 2 multiple curves are given because each of those is obtained for different numbers of stations providing τ as time passes during the seismic event.

To visualize how estimations of specific PGA values evolve with time, in Figure 3a the exceedance probabilities are given for different possible values of PGA_c of Eq. (8). The plots in the figure refer to 100 averaged simulations (i.e., the τ measurements were simulated 100 times for the same earthquake). It appears the probability of exceedance does not change after 10 sec – 13 sec, i.e., after on average 11-18 stations have measured τ.

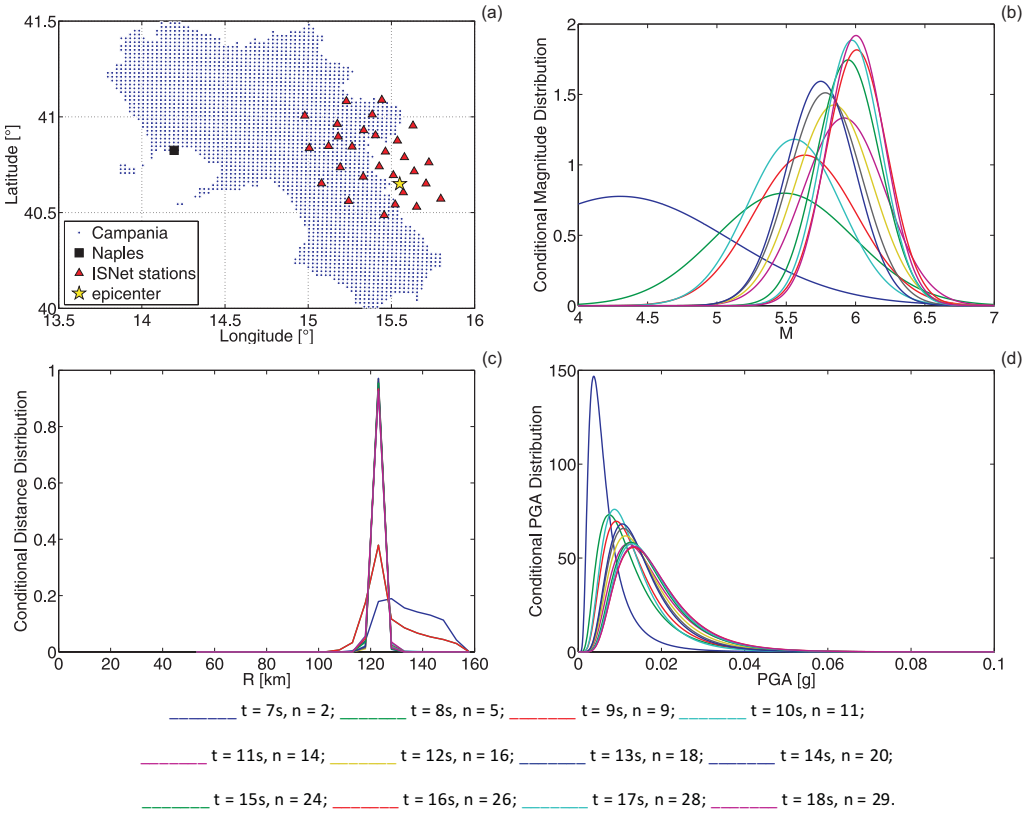

Figure 2. Results of RTPSHA for Naples in the case of a simulated M 6 event (adapted from Iervolino et al., 2009).

Figure 3a shows that there is a trade-off between the lead-time and the level of information based on which the alarm issuance is decided. Consequently, different lead-times may be considered, each of those corresponds to a different number (k) of stations providing τ. The average lead-times for the Campania region corresponding to the case when k equals 4, 18 or 29 were computed in Iervolino et al. (2009) for randomly occurring epicenters in the area covered by the INSnet system. In Figure 4 the map corresponding to 18 stations is given as analyzed with respect to a list of possible real-time risk reduction actions. Finally, in Figure 3b the coefficient of variation (CoV, the ratio of the standard deviation to the mean) of the PGA is given, as the number of stations providing τ increases. In particular, the CoV is computed, using Eq. (7), in the following cases: (i) considering both PDFs of M and R; (ii) considering only the modal value of the distance (R^*) from the PDFs of Figure 2c, in place of its full PDF; and (iii) considering only the mode of R and the maximum likelihood value of the magnitude, $\overline{M}$, in place of its full PDF. Note that in the case (iii) the real-time hazard is simply given by $f\left(im|\overline{M},R^*\right)$, i.e., the distribution of the PGA from the attenuation law computed for the specific $\left\{\overline{M},R^*\right\}$ pair. It appears from the results that the uncertainty of the distance is negligible with respect to the prediction of PGA as the CoV is almost the same considering whether there is or isn't uncertainty on distance (green and blue curves are overlapping); also uncertainty of magnitude, although larger than distance, is small if compared to that of the attenuation law. This conclusion holds stronger when several τ measures are available.

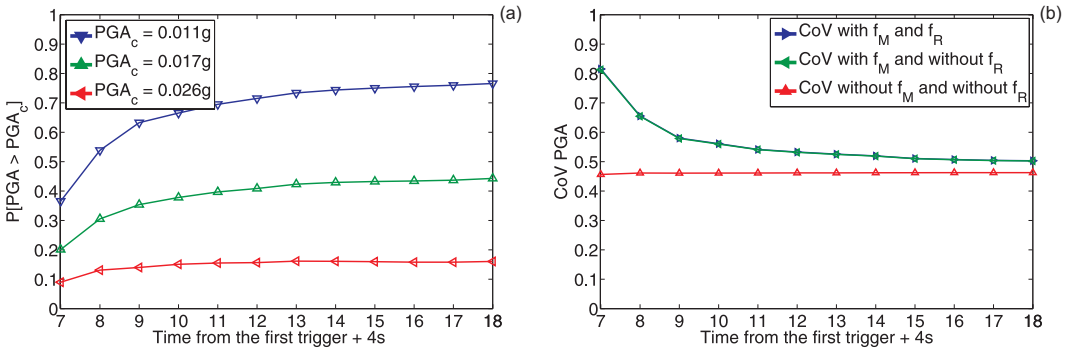

Figure 3. RTPSHA uncertainty analysis' results (adapted from Iervolino et al., 2009).

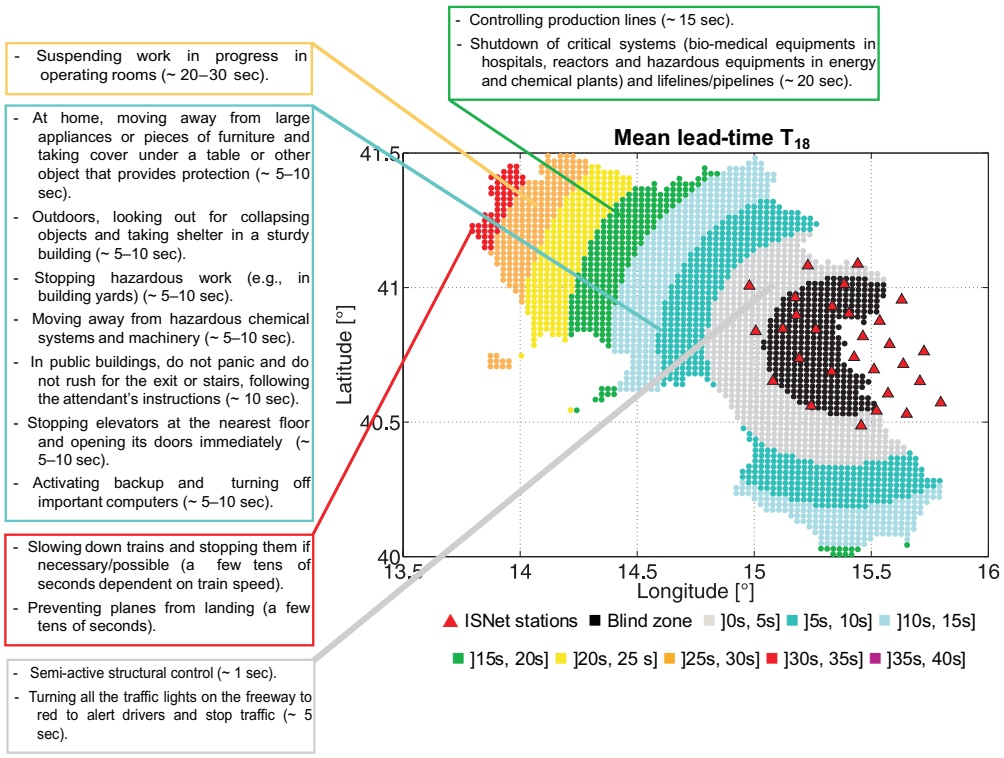

Figure 4. 18-stations lead-time map and possible risk-reduction actions (adapted from Iervolino et al., 2009).

2.2 *The false alarm issue in RTPSHA-based EEW*

A common way to evaluate the efficiency of a control system is the analysis of the false and missed alarms rates (Iervolino et al., 2006). According to the decisional rule of Eq. (8) a false alarm occurs when the alarm is issued while the intensity measure at the site PGA_T (T subscript means "true", indicating the realization of the PGA to be distinguished from the prediction PGA_C) is smaller than the threshold PGA_C. A missed alarm corresponds to do not launch the alarm when it is, in fact, needed, Eq. (9).

$$\begin{aligned} &Missed\ Alarm: \{No\ Alarm \cap PGA_T > PGA_C\} \\ &False\ Alarm: \{Alarm \cap PGA_T \le PGA_C\} \end{aligned} \tag{9}$$

It has been discussed above how the information and the uncertainties on earthquake location and magnitude are dependent on the number of stations triggered at a certain time. Therefore, in principle, the decisional rule may be checked at any time since the first station has triggered and, consequently, also the false and missed alarm probabilities are time dependent. Figure 5 reports the missed (MA) and false alarm (FA) probabilities as a function of time from the first trigger for the three PGA_C values according to which Figure 3a was computed.

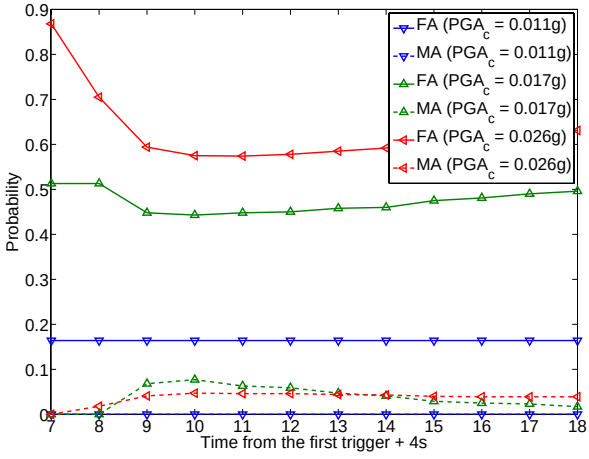

Figure 5. False and missed alarm probabilities for the PGA_C values and event of Figure 3a.

3 ERGO: A PROTOTYPAL EEW TERMINAL.

ERGO (EaRly warninG demO) is a visual terminal developed to test the potential of hybrid EEWSs (Festa et al., 2009). The system was developed by staff of the RISSC lab (www.rissclab.unina.it) and of the Department of Structural Engineering of the University of Naples Federico II (www.dist.unina.it) under the umbrella of AMRA scarl (www.amracenter.com). It was installed in the office of the dean of the school of engineering of the University of Naples Federico II on July 25 2008 and continuously operates since then.

ERGO processes in real-time the accelerometric data provided by a sub-net of ISNet and it is able to perform RTPSHA and eventually to issue an alarm in the case of events occurring with magnitude larger than 3 in the southern Appennines region. ERGO is composed of four panels (Figure 6):

1. ***Real-time monitoring and event detection***
   In this panel two kind of data are given: (a) the real-time accelerometric signals of the stations associated to the EEW terminal, shown on a two minutes time window; and (b) the portion of signal that, based on a signal-to-noise ratio determined the last trigger (i.e., event detection) for a specific station (on the left). Because it may be the case that local noise (e.g., traffic or wind) determine a station to trigger, the system declares an event (M larger than 3) only if at least three station trigger within the same two seconds time interval;

2. ***Estimation of earthquake parameters***
   This panel activates when the first panel declares an event. If this condition occurs the magnitude and location are estimated in real-time as a function of evolving information from the first panel. Here the expected value of the magnitude as a function of time from the origin of the detected event and the associated standard error are given. Moreover, on a map where also the stations are located, it shows the estimated epicenter, its geographical coordinates and the origin time;

3. ***Lead-time and peak-shaking map***
   This panel shows the lead-time associated to S-waves for the propagating event in the whole region. As a further information, on this panel the expected PGA on rock soil is given on the same map. As per the second panel, this one activates only if an event is declared from panel 1 and its input information come from panel 2.

4. ***RTPSHA and alarm issuance decision***
   This panel performs RTPSHA for the site where the system is installed based on information on magnitude and distance from panel 2. In particular, it computes and shows real-time evolving PDFs of PGA at the site. Because a critical PGA value has been established for the site (arbitrarily set equal to 0.01g) the system is able to compute the risk this PGA is exceeded conditional to the estimates for the ongoing event as a function of time. If such a risk exceeds 20%, i.e., the decisional rule of Eq. (8), the alarm is issued and a otherwise green light turns into red. This panel also gives, as summary information, the actual risk that the critical PGA value is exceeded along with the lead-time available from the site and the false alarm probability as per Eq. (9).

Figure 6 refers to a real event detected and processed in real-time by ERGO on November 19 2008. The system estimated the event as a M 3.1 earthquake located close to Potenza (capital of the Basilicata region), with an epicenter 115km far from the site. Because the event was a low-magnitude large-distance one, the risk the PGA_C could be exceeded was negligible and the alarm was, correctly, not issued.

Finally, note that ERGO is a visual panel only for demonstration and testing purposes, but it may be virtually ready be connected to devices for real-time risk reduction actions.

4 A LOSS-BASED APPROACH TO EEW

After presenting RTPSHA, it is worth a brief discussion on how magnitude and distance distributions conditional to the measurements of the seismic network can also be used for a real-time estimation of the risk which includes the expected losses from the impending earthquake (Iervolino et al., 2007). In fact, if an EEWS exists, in the framework of PBEE, the estimation of the expected losses for a specific building may be computed as in Eq. (10).

$$E\left[L \mid \underline{\tau}, \underline{s}\right] = \int_{L}\int_{DM}\int_{EDP}\int_{IM} l\, f\left(l \mid dm\right) f\left(edp \mid im\right) \times \\ \times f\left(im \mid \underline{\tau}, \underline{s}\right) dL\, dDM\, dEDP\, dIM \tag{10}$$

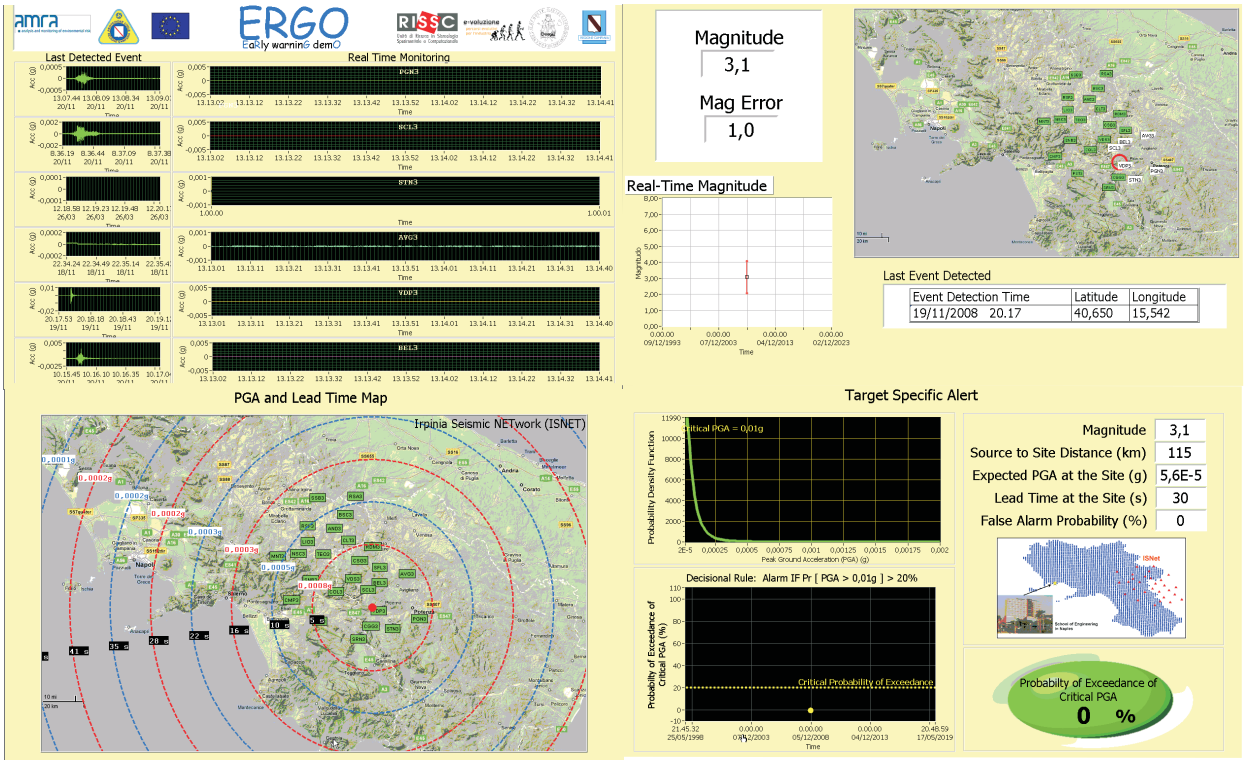

Figure 6. The ERGO EEW terminal.

Where $f(l|dm)$ is the PDF of the loss (L) given the structural and non-structural damage (DM); $f(dm|edp)$ is the PDF of damages given the Engineering Demand Parameters (EDP), proxy for the structural response; $f(edp|im)$ is the PDF of the EDPs conditioned to appropriate ground motion intensity measures (IM); $f(im|\underline{\tau},\underline{s})$ is the real-time hazard conditional to the real-time information, i.e., from Eq. (7).

To estimate the expected loss in the case of a warning, $E^{W}[L|\underline{\tau},\underline{s}]$, or no warning, $E^{\overline{W}}[L|\underline{\tau},\underline{s}]$, it is sufficient to modify Eq. (10) via $f(l|dm)=f^{W}(l|dm)$, which is the loss function reflecting a loss reduction action following the alarm, or $f(l|dm)=f^{\overline{W}}(l|dm)$, which is the loss function in the case of no warning, i.e., no security action is initiated.

Being able to compute, before the ground motion hits the structure, both the expected losses in case of warning or not, is relevant for taking the optimal decision, which is: to alarm only if this reduces the expected losses Eq. (11).

$$If:\begin{cases} E^{W}[L|\underline{\tau},\underline{s}] \le E^{\overline{W}}[L|\underline{\tau},\underline{s}] \Rightarrow not\ to\ alarm \\ E^{W}[L|\underline{\tau},\underline{s}] > E^{\overline{W}}[L|\underline{\tau},\underline{s}] \Rightarrow to\ alarm \end{cases} \tag{11}$$

This is better with respect to the decisional rule of Eq. (8) because it implicitly accounts for the costs of false and missed alarms. In fact, computing and comparing the expected losses, conditional to the real-time information coming from the EEWS in the case of alarming or not, allows the determination of the alarm threshold above which is convenient to issue the warning according to the *maximum optimality criterion*.

As an example, this approach was applied to a single-storey single-bay building supposed to host a school classroom (Figure 7, left) and equipped with a ringer activated by the EEWS. If the occupants are properly trained, in the case of an alarm the security action could consist of to shelter people below the desks. Three kind of losses can be considered in this case:

1. Casualties because of structural collapse in the case of an earthquake;
2. Injuries and casualties because of collapse of non-structural elements (e.g., the lighting system) in the case of an earthquake;
3. Costs of school downtime in the case of a false alarm.

In Figure 7 (right) are given the two curves representing the expected losses as a function of the geometric mean, $\hat{\tau}$, of the measurements. It is easy to recognize that the optimal alarm threshold is the value separating the region where to alarm is not convenient to that where to alarm implies a lower expected loss.

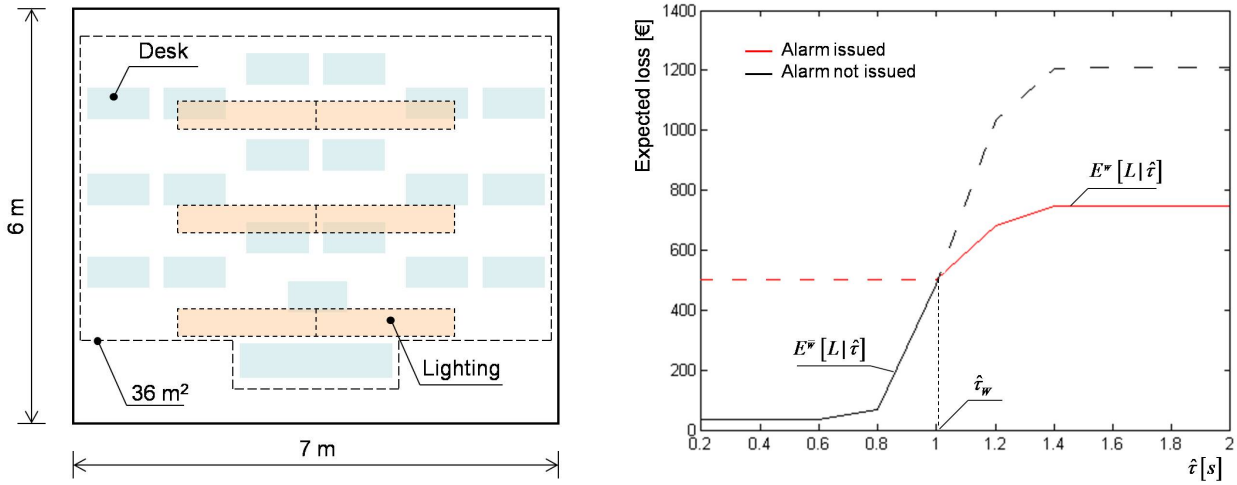

Figure 7. Expected loss-based alarm threshold (right) for a specific classroom (left) (adapted from Iervolino et al., 2007).

5 CONCLUSIONS

In this paper a brief review of the issues associated to the real-time adaption of PSHA and PBEE for earthquake early warning purposes are given. It was shown how the hazard integral can incorporate the information provided by a seismic network about a developing earthquake and how it results in time-dependent hazard curves which may be used for automated decision making also controlling the false and missed alarm rates and lead-time. The approach of RTPSHA can be extended further to compute the expected loss as a function of the EEWS information. This may help in taking the optimal decision in the framework of real-time risk management for a specific structure equipped with an EEWS.

A prototypal EEW terminal based on the seismic network installed in the Irpinia region in southern Italy was also presented.

In conclusion, it is to note the way RTPSHA works may seem odd. In fact, to estimate, from early signals, the source parameters to be plugged in an attenuation law for ground motion predictions at other sites is appropriate for classic hazard analysis. On the other hand, one can argue that going back to the source is a step not strictly required which adds uncertainty, and that it would be preferable to use the signals recorded in real-time by the network in the area where the earthquake is developing to directly predict the peak motion at other distant sites. Unfortunately, tools to operate EEWSs in this way are not readily available. Therefore, although the very large uncertainty of the attenuation law dominates those related to the estimation of magnitude and source-to-site distance, the RTPSHA seems to be currently the best option for engineering applications of EEW.

ACKNOWLEDGEMENTS

The support from the SAFER (EU's Sixth Framework Programme, contract 036935) and ReLUIS (Italian Department of Civil Protection, 2005-2008) research projects is gratefully acknowledged.

Efforts of co-workers who have contributed importantly to the results reported here may be not adequately reflected by the references below.

REFERENCES

Allen R.M., Kanamori H. (2003) The potential for earthquake early warning in southern California. *Science,* 300:786–789.

Convertito V., Iervolino I., Giorgio M., Manfredi G., Zollo A. (2008) Prediction of response spectra via real-time earthquake measurements. *Soil Dyn Earthquake Eng*, 28:492–505.

Cornell CA. (1968) Engineering seismic risk analysis. *Bull Seism Soc Am*, 58:1583–606.

Festa G., Martino C., Lancieri M., Zollo A., Iervolino I., Elia L., Iannaccone G., Galasso C. (2009) ERGO: a visual tool for testing earthquake early warning systems. (in preparation)

Iervolino I., Convertito V., Giorgio M., Manfredi G., Zollo A. (2006) Real-time risk analysis for hybrid earthquake early warning systems. *Journal of Earthquake Engineering*, 10:867–885.

Iervolino I., Giorgio M., Manfredi G. (2007) Expected loss-based alarm threshold set for earthquake early warning systems. *Earthquake Engn Struct Dyn*, 36:1151–1168.

Iervolino I., Giorgio M., Galasso G., Manfredi G. (2009) Uncertainty in early warning predictions of engineering ground motion parameters: what really matters? *Geophysical research letters,* 36, L00B06 doi:10.1029/2008GL0366449.

Sabetta F., Pugliese A. (1996) Estimation of response spectra and simulation of nonstationarity earthquake ground motion. *Bull Seism Soc Am*, 86:337–352.

Satriano C., Lomax A., Zollo A. (2008). Real-time evolutionary earthquake location for seismic early warning, *Bull Seism Soc Am*, 98:1482–1494.

Weber E., Convertito V., Iannaccone G., Zollo A., Bobbio A., Cantore L., Corciulo M., Di Crosta M., Elia, L. Martino, C. Romeo A., Satriano C. (2007) An advanced seismic network in the southern Apennines (Italy) for seismicity investigations and experimentation with earthquake early warning. *Seism Res Lett,* 78:622-634.